A New Active Clamp Forward Converter Using Secondary Inductor Current Ripple for Improved ZVS Operation

Sung-Sae Lee, Sang-Kyoo Han and Gun-Woo Moo

Department of Electrical Engineering and Computer Science,
Korea Advanced Institute of Science and Technology,
373-1 Guseong-Dong, Yuseong-Gu, Daejeon, 305-701, Republic of Korea
Phone: +82-42-869-3475, Fax: +82-42-861-3475
E-mail: gwmoon@ee.kaist.ac.kr

Abstract

A new asymmetrical zero voltage switching (ZVS) active clamp forward converter is proposed. Since the ripple current of secondary inductor plays a key role in the ZVS operation of main power switch, the proposed converter shows an excellent ZVS performance. The synchronous rectification is employed to reduce the rectification loss. The operational principle and ZVS analysis are presented. Experimental results demonstrate that the proposed converter can achieve an excellent ZVS performance throughout all load conditions and the significant improvement in the efficiency for the 100W(5V, 20A) prototype converter

1. Introduction

The continuous demand of high efficiency and high power density DC/DC power modules for the distributed power systems of sever and telecommunication application derives a need for new power processing techniques and circuit topologies. Among them, since resonant circuits [1-2] can achieve the zero voltage switching (ZVS) of power switches, they show the reduced switching loss and low EMI noise. However, they have an inherent disadvantage of high voltage and/or current stresses on semiconductors, which result in higher conduction loss compared to the pulse width modulation (PWM) converters. Therefore, the power processing technology has been changed to combine the simplicity of PWM converters with the soft-switching characteristics of resonant converters. This allows resonant zero voltage switching of power switches while the power is controlled be PWM method. The active clamp forward converter [3-5], which can achieve the ZVS operation of both switches, is widely used. However, the ZVS operation of the main switch is very difficult compare to the auxiliary clamp switch since it uses only small leakage inductor current to achieve the ZVS operation. The simplest technique to achieve ZVS operation of main power switch is to increase the magnetizing current by reducing the magnetizing inductor. However, the large magnetizing current causes serious conduction loss in the transformer and power switches.

In order to solve these drawbacks, this paper proposes a new active clamp ZVS PWM forward converter. As shown in Fig.1, the structure of the proposed converter is similar to that of the active clamp forward converter. However, the polarity of the transformer is reversed like that of the flyback converter. Since the secondary inductor current ripple plays a key role in the ZVS operation of main power switch, the proposed converter shows an excellent ZVS performance.

The operational principles, ZVS analysis, and experimental results are presented to confirm the validity of the proposed converter.

2. Operational Principle

The circuit diagram of the proposed active clamp forward converter with improved ZVS performance is given in Fig. 1. Fig. 2 shows the key operating waveforms of the proposed converter in the steady state. Each switching period is subdivided into eight modes. In order to illustrate the steady state operation, several assumptions are made as followings:

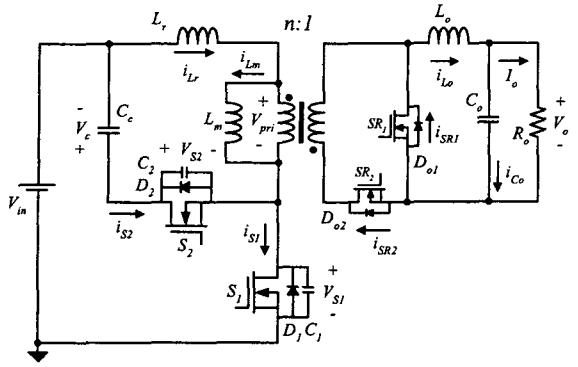

Fig. 1 Circuit diagram of the proposed converter

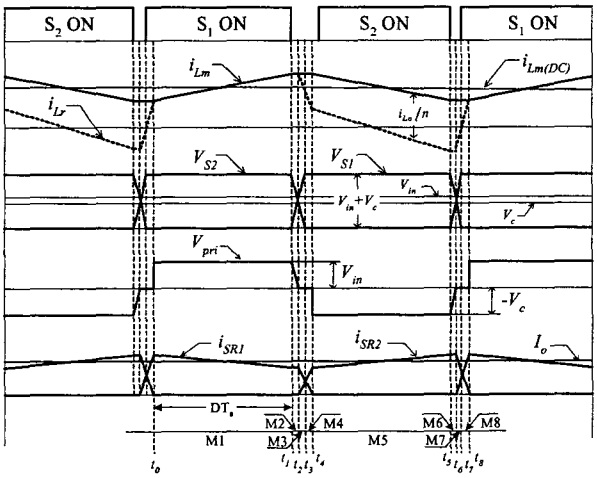

Fig. 2 Key waveforms for the mode analysis

(a) The switches, S_1 and S_2, are ideal expect for their internal diode and output capacitor.

(b) The output voltage $V_o(t)$ and clamping capacitor voltage $V_c(t)$ are assumed to be constant, V_o and V_C, respectively.

(c) The transformer magnetizing current $i_{Lm}(t)$ is assumed to be constant during the time intervals $t_1 \sim t_2$ and $t_5 \sim t_6$.

(d) The output capacitors of switches, C_1 and C_2, have the same value of C_S.

Mode 1 $(t_0 \sim t_1)$: Mode 1 begins when the commutation of $i_{SR1}(t)$ and $i_{SR2}(t)$ is completed. Then $i_{Lo}(t)$ flows through C_o and SR_1. Since S_1 is on and S_2 is off state, V_{in} is applied to $L_m + L_r$. $i_{Lm}(t)$ and $i_{Lo}(t)$ can be expressed as follows:

$$i_{Lm}(t) = \frac{V_{in}}{L_m + L_r} t + i(t_o) = i_{Lr}(t) = i_{S1}(t) \tag{1}$$

$$i_{Lo}(t) = -\frac{V_o}{L_o} t + i_{Lo}(t_0) = i_{SR2}(t) \tag{2}$$

where

$$i_{Lm}(t_0) = \frac{I_o}{n} - \frac{\triangle i_{Lm}}{2} = \frac{I_o}{n} - \frac{V_{in}}{2(L_m + L_r)} DT_s$$

$$i_{Lo}(t_0) = I_o + \frac{\triangle i_{Lo}}{2} = I_o + \frac{V_o}{2L_o} DT_s.$$

Mode 2 $(t_1 \sim t_2)$: This mode begins when S_1 is turned off. Until $V_{S1}(t)$ is lower than V_{in}, the dotted end of the transformer's primary side is positive with respect to the undotted end of that and diode D_{o2} is still reverse biased. Therefore, C_1 and C_2 are linearly charged and discharged by $i_{Lm}(t)$ respectively. From the assumption (c), $V_{S1}(t)$ can be expressed as follows:

$$V_{S1}(t) = \frac{i_{Lm}(t_1)}{2C_s} t \tag{3}$$

where

$$i_{Lm}(t_1) = \frac{I_o}{n} + \frac{V_{in}}{2(L_m + L_r)} DT_s.$$

Mode 3 $(t_2 \sim t_3)$: After $V_{S1}(t)$ increases to V_{in}, $i_{Lo}(t)$ begins to freewheel through D_{o1} and D_{o2}. Since the primary voltage across the transformer is 0V, C_1 and C_2 are charged and discharged in a resonant manner of L_r and $C_1 + C_2 = 2C_s$, respectively. $i_{Lr}(t)$ and $V_{S1}(t)$ can be expressed as follows:

$$i_{Lr}(t) = i_{Lm}(t_2) \cos\left(\sqrt{\frac{1}{2L_r C_s}} t\right) \tag{4}$$

$$V_{S1}(t) = i_{Lm}(t_2) \sqrt{\frac{L_r}{2C_s}} \sin\left(\sqrt{\frac{1}{2L_r C_s}} t\right) + V_{in}. \tag{5}$$

Mode 4 $(t_3 \sim t_4)$: After $V_{S1}(t)$ and $V_{S2}(t)$ reach $V_{in} + V_c$ and 0V, respectively, $i_{Lr}(t)$ flows through D_2 and the zero voltage across S_2 is maintained. Since D_{o1} and D_{o2} are still conducting, the voltage across the transformer is 0V and $-V_c$ is all applied to L_r. Therefore, $i_{Lr}(t)$ rapidly decreases as follows:

$$i_{Lr}(t) = -\frac{V_c}{L_r} t + i_{Lr}(t_3) \tag{6}$$

where

$$i_{Lr}(t_3) = \sqrt{i_{Lm}^2(t_2) - \frac{2C_S V_c^2}{L_r}}$$

which can be derived form equation (4) and (5).

Mode 5 $(t_4 \sim t_5)$: When $i_{Lr}(t)$ reaches $i_{Lm}(t_4) - i_{Lo}(t_4)/n$, $i_{Lo}(t)$ complete its freewheeling and SR_2 and SR_1 are turned on and off, respectively, with

D_2 still conducting. Since $-V_c$ is applied to $L_m + L_r$ and $V_c/n - V_o$ is applied to L_o, $i_{Lm}(t)$, $i_{Lo}(t)$ and $i_{Lr}(t)$ can be expressed as follows:

$$i_{Lm}(t) = -\frac{V_c}{L_m + L_r}t + i_{Lm}(t_4) \quad (7)$$

$$i_{Lo}(t) = \frac{\frac{V_c}{n} - V_o}{L_o}t + i_{Lo}(t_4) \quad (8)$$

$$i_{Lr}(t) = i_{Lm}(t) - \frac{i_{Lo}(t)}{n}. \quad (9)$$

Since S_2 can be turned on before $i_{Lr}(t)$ decreases to zero, the ZVS of S_2 can be easily achieved like that of the active clamp forward converter.

Mode 6 *($t_5 \sim t_6$)* : When S_2 is turned off, C_1 and C_2 are discharged and charged, respectively, by $i_{Lr}(t_5)$ until $V_{S2}(t) \le V_c$. $V_{S2}(t)$ can be expressed as follows:

$$V_{S2}(t) = \frac{\frac{i_{Lo}(t_5)}{n} - i_{Lm}(t_5)}{2C_s}t. \quad (10)$$

Mode 7 *($t_6 \sim t_7$)* : After $V_{S2}(t)$ increases over V_c, $i_{Lo}(t)$ begins to freewheel through D_{o1} and D_{o2}. Then, C_1 and C_2 are discharged and charged in a resonant manner of L_r and $C_1 + C_2 = 2C_s$. Therefore, $i_{Lr}(t)$ and $V_{S2}(t)$ can be expressed as follows:

$$i_{Lr}(t) = \left(i_{Lm}(t_6) - \frac{i_{Lo}(t_6)}{n}\right)\cos\left(\sqrt{\frac{1}{2L_rC_s}}t\right) \quad (11)$$

$$V_{S2}(t) = \sqrt{\frac{L_r}{2C_s}}\left(\frac{i_{Lo}(t_6)}{n} - i_{Lm}(t_6)\right)\sin\left(\sqrt{\frac{1}{2L_rC_s}}t\right) + V_c \quad (12)$$

It is noted that the current for the ZVS of S_1 is only $\Delta i_{Lm}/2$ in active clamp forward converter. Therefore, it is hard to satisfy the ZVS condition of S_1. However, in the proposed converter, the current for the ZVS of S_1 is $(\Delta i_{Lm} + \Delta i_{Lo}/n)/2$. Therefore, ZVS condition of S_1 is easily achieved. The detailed analysis of the ZVS operation is described in the next section.

Mode 8 *($t_7 \sim t_8$)* : After $V_{S1}(t)$ and $V_{S2}(t)$ reach 0V and $V_{in} + V_c$, respectively, S_1 is turned on. Since $i_{Lo}(t)$ is still freewheeling through D_{o1} and D_{o2}, V_{in} is all applied to L_r. $i_{Lr}(t)$ can be expressed as follows:

$$i_{Lr}(t) = \frac{V_{in}}{L_r}t + i_{Lr}(t_7) \quad (13)$$

where

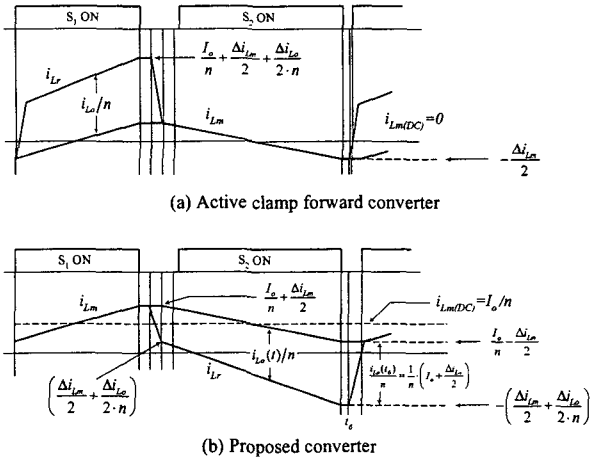

Fig. 3 Comparative analysis of the ZVS currents

$$i_{Lr}(t_7) = \sqrt{\left(i_{Lm}(t_6) - \frac{i_{Lo}(t_6)}{n}\right)^2 + \frac{2C_sV_{in}^2}{L_r}}.$$

After the end of mode 8, the operation form t_0 to t_8 is repeated.

3. ZVS Current Analysis

In this section, the ZVS current analysis of the proposed converter is accomplished. In order to achieve the ZVS of the power switch, the energy stored in the inductor should be greater than the energy stored in the output capacitor of the power switch. Since the energy stored in the inductor is mainly determined by the current flows through it, it is critical to guarantee the large inductor current at the switching time without any additional losses to achieve the ZVS of the power switch. Fig. 3 shows the magnetizing current and the leakage inductor current of the active clamp forward converter and those of the proposed converter. In active clamp forward converter, the ZVS condition of clamp and main power switches can be expressed, respectively, as follows:

$$\frac{1}{2}L_r\left(\frac{I_o}{n} + \frac{\triangle i_{Lm}}{2} + \frac{\triangle i_{Lo}}{2n}\right)^2 \ge \frac{1}{2}(2C_s)(V_{S2}/2)^2 \quad (14)$$

$$\frac{1}{2}L_r\left(\frac{\triangle i_{Lm}}{2}\right)^2 \ge \frac{1}{2}(2C_s)(V_{S1}/2)^2. \quad (15)$$

As described in equation (14), the ZVS of the clamp power switches easily achieved due to the large inductor current. However the ZVS of the main power switch is very difficult due to the small magnetizing current as shown in equation (15) and Fig. 3(a). The ZVS condition of clamp and main power switches of the proposed converter can be

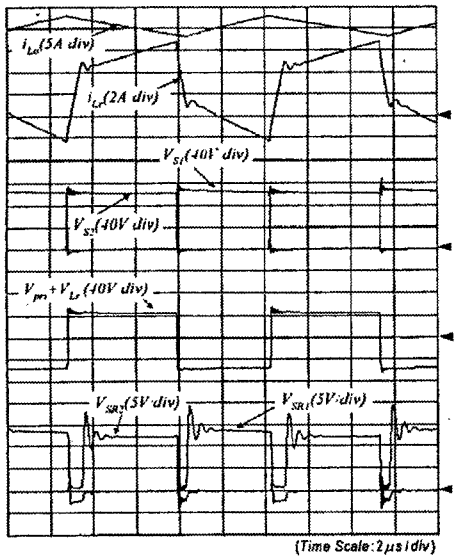

Fig. 4 Key experimental waveforms at full load

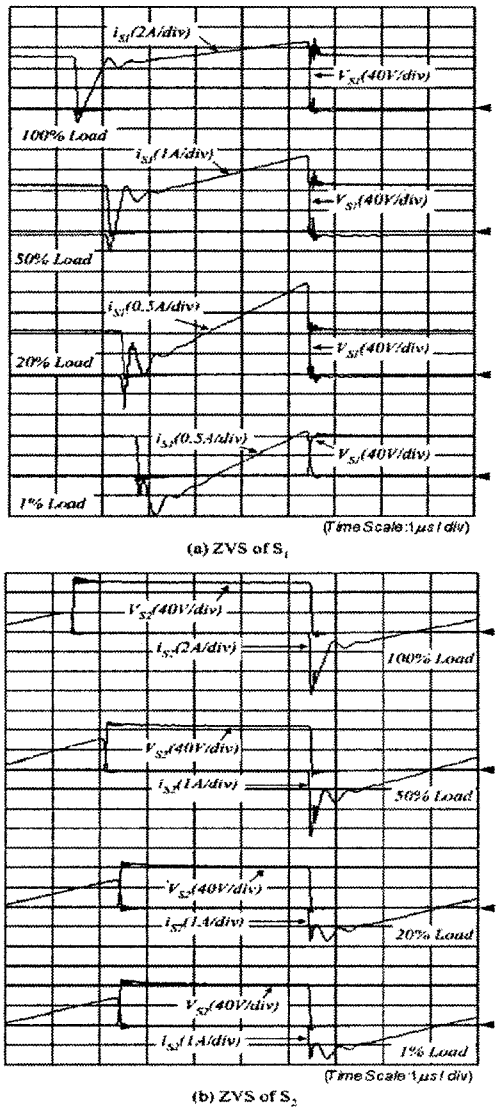

Fig. 5 ZVS waveforms with the load variations

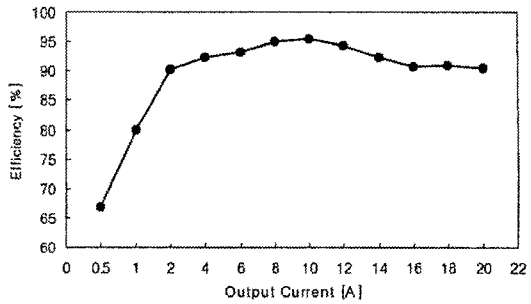

Fig. 6 Efficiency under the load variations

Table 1 Components list

Switching frequency (f_s)	100kHz
Switches (S_1, S_2)	IRF3315
Synchronous rectifiers (SR_1, SR_2)	IRF3703
Output inductance (L_o)	6 μH
Leakage inductance (L_r)	1.5 μH
Magnetizing inductance (L_m)	78 μH
Transformer turn ratio (n:1)	4:1
Clamping Capacitor (C_c)	2.2 μF
Output capacitor (C_o)	1000 μF

expressed, respectively, as follows:

$$\frac{1}{2}L_r\left(\frac{I_o}{n}+\frac{\triangle i_{Lm}}{2}\right)^2 \geq \frac{1}{2}(2C_s)(V_{S2}/2)^2 \qquad (16)$$

$$\frac{1}{2}L_r\left(\frac{\triangle i_{Lm}}{2}+\frac{\triangle i_{Lo}}{2n}\right)^2 \geq \frac{1}{2}(2C_s)(V_{S1}/2)^2. \qquad (17)$$

As described in equation (16), the ZVS of the clamp power switch of the proposed converter is easily achieved due to the large inductor current. In addition, since the reflected ripple current of the output inductor is added to the magnetizing current as shown in equation (17) and Fig. 3(b), the ZVS of the main power switch can also be easily achieved. Therefore, the proposed converter shows better ZVS performance than active clamp forward converter

4. Experimental Results

To validate the characteristics of the propose converter, a prototype of a 5V, 100W converter constructed using the components as shown in Ta 1. Fig. 4 shows key waveforms of the propc converter at full load condition. $i_{Lo}(t)$ has 4A ri current and $i_{Lr}(t)$, $V_{S1}(t)$ and $V_{S2}(t)$ are well a

with the theoretical waveforms of Fig. 2. The voltage across SR_2, $V_{SR2}(t)$, is used as the gate signal for SR_1 and $V_{SR1}(t)$ is used as the gate signal for SR_2. Fig. 5 shows the voltage and current of S_1 and S_2 at the different load conditions. As previously mentioned, since the reflected ripple current of output inductor is added to the magnetizing current, the ZVS of S_1 can be easily achieved from full load to very light load as shown in Fig. 5(a). The ZVS of S_2 is also easily achieved as the same manner of the active clamp forward converter as shown in Fig. 5(b). Fig. 6 shows the efficiency of the proposed converter according to the load variation. As expected, the high efficiency can be obtained around 90.46% at full load and the maximum efficiency becomes approximately 95.5%. This high efficiency indicates the significant reduction of the switching losses for the entire load ranges by employing the new ZVS scheme of the proposed converter. It is concluded that the proposed converter can effectively achieve the ZVS of all switches without any auxiliary circuits.

5. Conclusions

This paper presented the analysis and experimental results of a new active clamp forward converter. The ZVS operation of the main switch is easily achieved due to the effect of the reflected ripple current of the output inductor from no load to full load conditions without any auxiliary circuits. Therefore, high efficiency and low EMI noise can be maintained through all load conditions. The operational principles and ZVS current analysis have been presented and prototype converter is built and tested. The experimental results of a 100W prototype converter prove the key characteristics of the proposed converter. The efficiency of the proposed converter is obtained 90.46% at the full load condition and a maximum efficiency becomes 95.5% around half load condition. Therefore, the proposed converter is suitable for server and telecommunication equipments that require high efficiency, high power density, and low EMI noise with 48V bus voltage

References

[1] K. H. Liu and F. C. Lee, " Zero-voltage switching technique in DC/DC converters", IEEE Trans. Power Electronics, Vol. 6, July 1990, pp. 293-304

[2] J. A. Cobos, O. Garcia, J. Uceda, J. Sebastian and E. de la Cruz, "Comparison of high efficiency low output voltage forward topologies", in Proc. IEEE PESC, Vol. 2, June 1994, pp. 887-894

[3] H. K. Ji and H. J. Kim, "Active clamp forward converter with MOSFET synchronous rectification", in Proc. IEEE PESC, Vol. 2, June 1994, pp. 895-901

[4] M. Jinno, Jiann-Chem Sheen and Po-Yuan Chen, " Effect of magnetizing inductance on active-clamped forward converters", in Proc. INTELEC, October 2003, pp. 636-642

[5] V. Tuomainen and J. Kyyra, " Effect of resonant transition on efficiency of forward converter with active clamp and self-driven sr's", in Proc. IEEE PESC, Vol. 3, June 2003, pp. 1333-1338